Macromolecules **2006,** *39,* 1779−1789

Dielectric Study of Dynamic Heterogeneity in Miscible Blends of Polyethers and Poly(vinylethylene)

Yuji Hirose[†] and Keiichiro Adachi*

Department of Macromolecular Science, Graduate School of Science, Osaka University, Toyonaka, Osaka 560-0043, Japan

Received October 12, 2005; Revised Manuscript Received December 30, 2005

ABSTRACT: Dynamic heterogeneity in miscible blends was investigated by the use of dielectric relaxation spectroscopy for blends composed of poly(vinylethylene) (PVE) and various polyethers, i.e., poly(butylene oxide) (PBO), poly(isopropyl glycidyl ether) (PiPGE), poly(*n*-butyl glycidyl ether) (PnBGE), and poly(*tert*-butyl glycidyl ether) (PtBGE). All polyethers are type AB polymers and exhibit both the dielectric normal- and segmental-mode relaxations, but PVE exhibits only the segmental relaxation. The data indicate that the loss curves for the segmental relaxation of PVE/PBO blends are bimodal in the range of PBO content less than 0.25. Since the dielectric relaxation strength of PBO is much higher than that of PVE, unimodal loss curves are seen at high PBO content. The effective glass transition temperatures for the fast and slow modes estimated with the Lodge−McLeish model agree fairly well with the temperatures at which segmental relaxation times become ca. 100 s. The ratio of the relaxation times for the normal and segmental modes $\log(\tau_n/\tau_s)$ increases with increasing content of PVE. The correlation length of concentration fluctuation has been deduced to be 1.0 nm from the behavior of broadening of the relaxation spectra for the segmental and normal modes of PBO. In blends of polyethers such as PnBGE/PtBGE, the loss curves for the segmental modes are unimodal but are asymmetrical when the fraction of one component is 0.25 or 0.75. The asymmetrical loss curve can be attributed to the bimodal relaxation spectrum even though the loss curve is unimodal. The separation between the fast and slow modes in blends of the polyethers has been estimated by utilizing $\log(\tau_n/\tau_s)$ as a tool to estimate the location of the segmental loss peaks of the components.

Introduction

Understanding of molecular dynamics in blends of miscible polymers is an important issue of polymer physics. Until about 10 years ago, it was believed that miscible polymer blends exhibit single glass transition and a unimodal dielectric or mechanical loss curve.[1,2] It has been also known that the relaxation spectra of miscible blends become much broader than those of the components and that the time−temperature superposition principle does not hold.[3−6] Although this criterion for judging miscibility of a blend was adopted long, Alegria et al.[7] found that this criterion does not hold in miscible blends of *cis*-polyisoprene (PI) and poly(vinylethylene) (PVE) which exhibit bimodal dielectric loss curves for the local segmental relaxation (α relaxation). Similar dielectric behavior was observed for blends in which the difference of glass transition temperatures T_g of the components is larger than 70 K.[8−15] Dynamic heterogeneity was investigated by using methods other than dielectric spectroscopy, i.e., rheology,[16,17] NMR,[18−24] ESR,[25] neutron scattering,[12,26] and thermally stimulated depolarization current.[27] In those studies, the fast and slow modes due to the low- and high-T_g components, respectively, were observed. Such a behavior of distinct dynamics of the components has been also known for polymer/diluent systems.[28,29] However, Zhang et al.[30,31] reported that blends in which hydrogen bonds are formed between components exhibit unimodal α relaxation despite the large difference of T_g of the components. As is well-known, segmental dynamics is closely related to glass transition. Recently, Taniguchi et al.[32] observed a double stepwise increase of the heat capacity for the PS/toluene system by using an adiabatic calorimeter. Sakaguchi et al.[33] also observed bimodal behavior for the glass transition in PI/PVE blends. Thus, the dynamic heterogeneity can be also observed for glass transition of miscible blends.

Dynamic heterogeneity in the terminal chain dynamics of the components has been also investigated by measurements of rheology, diffusion, infrared dichroism, and dielectric relaxation.[14,15,22,24,34−43] Hirose et al. reported the dielectric normal mode relaxation of the PI chains in blends of PI/PVE.[14] It was found that the shape of the loss curve for the normal mode is independent of the composition, indicating the correlation length of concentration fluctuation is less than the dimension of the PI chain. The data for PI/PVE also indicate that the ratio $\log(\tau_s/\tau_n)$ of the segmental (τ_s) and terminal chain dynamics(τ_n) is almost independent of the composition.[14] However, the distinct temperature and composition dependences of the local and global motions are found in several blend systems.[22,24,34−43] He et al.[22,24] studied the monomeric friction coefficient for the global motions and the correlation time for the local segmental motions for PI/PS blends and found that the local segmental dynamics is heterogeneous but the terminal dynamics is homogeneous.

For pure polymers the temperature T dependences of the relaxation times for the segmental (τ_s) and terminal chain dynamics (τ_n) have been examined for various polymers with the dielectric method[44−47] and the rheological method.[48−50] The results of those studies show that the temperature dependences of segmental mode and terminal mode are different near T_g. However, $\log(\tau_s/\tau_n)$ becomes almost independent of temperature within the deviation of ±0.3 decades in the T range of $T > T_g + 30$ K.[44−48] It is stressed that in the present study was made in the latter temperature range satisfying the constancy of $\log(\tau_s/\tau_n)$. We will assume this constancy in the analyses of the blends although the relationship between segmental and terminal

---

* To whom correspondence should be addressed. E-mail: adachi@chem.sci.osaka-u.ac.jp.

[†] Present address: Venture Business Lab., Chiba University, Inage, Chiba 263-8522, Japan.

10.1021/ma052216x CCC: $33.50

dynamics in blends is more complex than that in pure polymers.

Several theories have been proposed to explain the dynamic heterogeneity in miscible blends.[9,51−53] Zetsche and Fischer[51] proposed a theory of the mechanism of broadening of the relaxation spectra of miscible blends considering Gaussian distribution of local concentration. Roland and Ngai[9] explained the broad relaxation spectra of PS/PVME blends using the coupling model. Kumar et al.[52] extended the Zetsche−Fischer model by considering cooperative volume. Chung et al.[18] proposed a self-concentration model to explain dynamic heterogeneity of a miscible blend. This model was developed by Lodge and McLeish.[53]

The studies of dynamic heterogeneity so far reported indicate that dynamic heterogeneity in miscible blends depends on the chemical structures of the components. Therefore, studies for more variety of miscible blends are needed. In this study we report the dynamic heterogeneity on blends composed of two polymers chosen from PVE and four kinds of polyethers, namely, poly(butylene oxide) (PBO), poly(isopropyl glycidyl ether) (PiPGE), poly(*n*-butyl glycidyl ether) (PnBGE), and poly(*tert*-butyl glycidyl ether) (PtBGE). These sample polymers have different T_gs ranging from 194 to 269 K, and our preliminary experiments indicate that they are miscible. Recently, we have reported the dielectric behaviors of these polyethers in the pure state.[47] In this paper we report both the segmental dynamics and the terminal chain dynamics of the components in the blends.

Blends used in this study are classified into two categories: one is the PVE/PBO system, and the other is the blends composed of the above-mentioned polyethers. In the former the dipole moment of PBO is much higher than that of PVE, and hence the dielectric spectra reflect only the dynamics of one component PBO in the range of weight fraction w_{PBO} of PBO larger than 0.25. We have also investigated the behavior of so-called dilute blends with $w_{\mathrm{PBO}} < 0.25$. In the blends of the second category, the dipole moments of the components are similar but T_gs are different. We will examine the effect of T_g difference of the components on the segmental dynamics.

Experimental Section

Materials. PVE was prepared by anionic polymerization of butadiene with *sec*-butyllithium (BuLi) in *n*-heptane containing a small amount of dipiperidinoethane (DPE) (DPE/BuLi molar ratio = 5/1) at 0 °C.[54] The polymerization reaction was terminated with methanol. All samples were precipitated by pouring heptane solutions in excess methanol and then dried under a vacuum. To prevent oxidation, the PVE samples were dissolved in benzene and added a small amount (ca. 0.1%) of 2,6-di-*tert*-butyl-4-methylphenol as the stabilizer. Then the benzene solutions were freeze-dried.

PBO, PiPGE, PnBGE, and PtBGE were prepared by ring-opening polymerization of corresponding epoxides by using potassium hydride as the initiator and 18-crown-6 as the catalyst in tetrahydrofuran.[55] All those reagents were purchased from Aldrich. Details of synthesis and characterization were reported previously.[47] Sample characteristics are shown in Table 1. All polyethers used in this study have structure represented as $-[\mathrm{CHR}-\mathrm{CH_2}-\mathrm{O}]_n-$, and the chemical structures of the side group R are represented as follows: PBO, $-\mathrm{CH_2CH_3}$; PiPGE, $-\mathrm{CH_2OCH(CH_3)_2}$; PiPGE, $-\mathrm{CH_2OCH(CH_3)_2}$; PiPGE, $-\mathrm{CH_2OCH(CH_3)_2}$; and PtBGE, $-\mathrm{CH_2OCH(CH_3)_3}$. The samples are perfectly amorphous, and no crystallization was observed by DSC.

Preparation of Blends and Their Miscibility. For all pairs of polymers listed in Table 1, the miscibility was tested by visual observation. The blends having the 50/50 composition were prepared by solution cast from THF solutions. We judged the miscibility of a pair of polymers by testing whether the blend was transparent or opaque; i.e., when the blend was opaque, the components were judged to be immiscible. The results are given in Table 2 in which "T" and "O" indicate "transparent" and "opaque", respectively. The blends judged to be miscible were further tested by DSC and confirmed that the blends exhibit a single glass transition. The DSC thermograms exhibit no peaks due to crystallization and melting. However, the data of the interaction parameters of these blends are not available at present.

Table 1. Weight-Average Molecular Weight M_w, Polydispersity Index M_w/M_n, and Glass Transition Temperature T_g of Polymer Samples

code	$10^{-3}M_w$	M_w/M_n	T_g
PVE-89	89	1.07	269
PVE-31	31	1.07	
PBO-4	4.1	1.20	
PBO-12	12.3	1.22	199
PBO-20	20.5	1.08	
PBO-50	50	1.31	199
PiPGE-22	22	1.55	206
PnBGE-25	25	1.49	194
PtBGE-21	21	1.57	249
PtBGE-37	37	1.79	249

Table 2. Miscibility of Blends with 50/50 Composition[a]

code	PVE	PBO	PiPGE	PnBGE	PtBGE
PVE	−	T	O	O	O
PBO		−	T	T	T
PiPGE			−	T	T
PnBGE				−	T
PtBGE					−

[a] O: opaque; T: transparent.

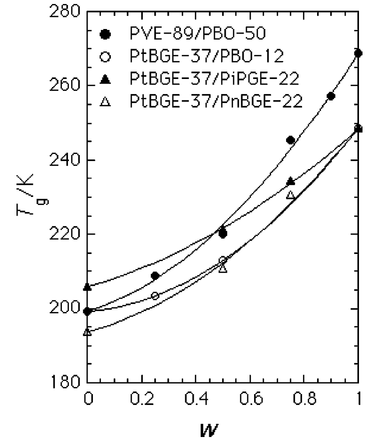

Figure 1. Dependences of T_g on the content *w* of PVE or PtBGE in the blends. The solid lines are the Kwei[57] equation (eq 1).

Glass Transition of Blends. Glass transition temperatures T_g of the blends of PVE/PBO, PnBGE/PtBGE, PBO/PtPGE, and PiPGE/PtBGE were measured by DSC (Seiko Instruments & Electronics Ltd., DSC-20, Japan) at a heating rate of 10 K/min and listed in Table 1. The dependences of T_g on the composition are plotted in Figure 1. All DSC curves around T_g were single sigmoid. A double-step increase of the heat capacity at T_g was not observed due to low sensitivity of the DSC.[32,33] The experimental T_gs do not conform to the familiar Fox equation[56] which predicts 7−9 K higher T_g than the observed one at $w = 0.5$. Therefore, we fitted the data to the Kwei[57] equation for blend composed of A and B:

$$T_g = \frac{(1-w)T_g^{\ A} + kwT_g^{\ B}}{(1-w) + kw} + qw(1-w) \qquad (1)$$

where *w* is the weight fraction of B and *k* and *q* are the parameters. The fitting parameters are listed in Table 3.

Dielectric Measurements. Measurements of relative dielectric constant ϵ' and dielectric loss factor ϵ'' were made by using two

Table 3. Parameters of Eq 1 for Blends

blends	k	q/K
PVE-89/PBO-50	1.00	−46.3
PtBGE-37/PBO-12	1.08	−47.0
PtBGE-37/PiPGE-22	1.00	−21.7
PtBGE-37/PnBGE-25	1.00	−34.3

RLC meters (QuadTech, models 1693 and 7600) in the frequency range from 10 Hz to 2 MHz. Details of the method were reported previously.[47] The capacitance cell and cryostat for measurements of viscous liquids were reported previously.[58] In some samples ϵ'' increased in the low-frequency region due to the ionic conductivity σ. We corrected the contribution $\epsilon''_\sigma = \sigma/(2\pi\epsilon_0 f)$, where ϵ_0 is the absolute dielectric constant of vacuum and f the frequency in Hz. First, σ was estimated by assuming that ϵ'' at the lowest frequency (10 Hz) was totally due to the ionic conduction. Then a slightly smaller value than thus-estimated σ was used in calculation of eq 1 to avoid overestimation of σ.

Results and Discussion

1. Dielectric Relaxations of PVE/PBO Blends. The dielectric behaviors of PVE/PBO blends were examined by using three PBO samples having different molecular weights (MW). When it was needed to erase the effect of the normal mode, a high-MW sample of PBO-50 exhibiting the normal mode relaxation in low-frequency/high-temperature regions was used. On the other hand, when we needed the data of both the segmental and normal modes, PBO-20 and PBO-4 were used.

PVE-89/PBO-50 Blends. Figure 2 shows the temperature dependences of ϵ'' for PVE-89/PBO-50 blends with various compositions. In this figure, the baselines are shifted upward by 0.06, 0.04, and 0.02 for the ϵ'' curves of blends with PVE contents of 50, 75, and 90 wt %, respectively. As mentioned above, PBO-50 exhibits the normal mode relaxation at high temperature, and hence the observed ϵ'' peak is due to the segmental mode relaxation of PBO and PVE. The gradual increase of ϵ'' in the range above 300 K is due to both the normal mode of PBO and ionic conduction. It is seen that the ϵ'' curves of blends with weight fraction of PVE $w_{\mathrm{PVE}} = 0.75$ and 0.90 are bimodal as indicated by the arrows, but in the range $w_{\mathrm{PVE}} < 0.75$ the ϵ'' curves are unimodal. Since the dielectric relaxation strength of PBO is much stronger than that of PVE, we can observe bimodal loss peaks only in the region where $w_{\mathrm{PVE}} > 0.75$. The relaxation processes corresponding to the high- and low-temperature loss peaks are designated the slow and fast modes, respectively. From the composition dependences of the intensities, the slow and fast modes can be assigned to PVE and PBO, respectively. It is noted that T_g difference (ΔT_g) between PVE and PBO is 70 K, which is similar to that of PVE/PI blends. However, in PVE/PI blends, the bimodal loss peak is observed in the PI (low-T_g component) rich region, in contrast to PVE/PBO blends.[7]

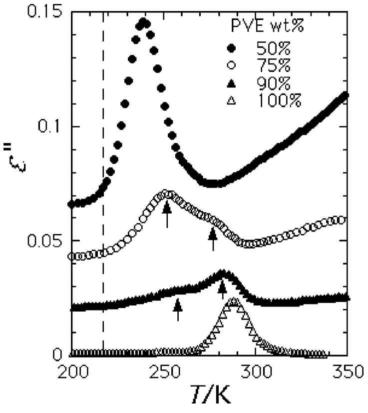

Figure 2. Temperature dependences of ϵ'' for PVE-89/PBO-50 blends at 1 kHz. The baselines are shifted upward by 0.06, 0.04, and 0.02 for the ϵ'' curves of blends with PVE contents of 50, 75, and 90 wt %, respectively. The dashed line indicates the temperature of loss peak of pure PBO at 1 kHz.

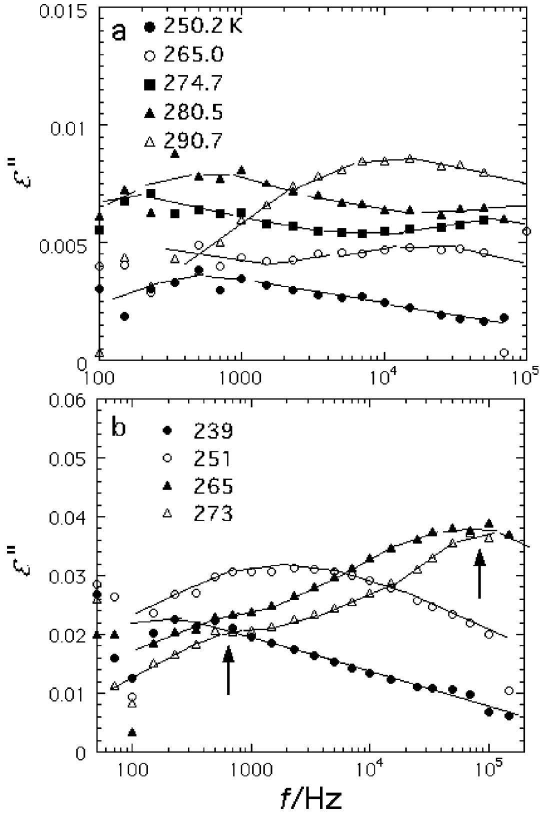

Figure 3. Frequency dependences of ϵ'' of (a) PVE-89/PBO-50 (90/10) blend and (b) PVE-89/PBO-50 (75/25) blend.

Figure 3a shows the frequency dependences of ϵ'' for PVE-89/PBO-50(90/10). Unfortunately, the noise level is high since the intensity of ϵ'' is low. Therefore, the data points obtained in the range from 100 Hz to 100 kHz where the S/N ratio is relatively high were used. In this figure we can see the loss peak due to the fast mode when $T < 250$ K. At $T = 275$ K the other loss peak due to the slow mode appears around 100 Hz and moves to high frequency with increasing T. The ϵ'' curves of the PVE-89/PBO-50 (75/25) blend also exhibit the bimodal loss peak composed of the fast and slow modes, as indicated by the arrows shown in Figure 3b. The relative intensity of the slow mode becomes low due to the increase of PBO content.

In Figures 2 and 3 the relative intensities of the fast and slow modes change with composition, supporting the assignments of the modes. The assignments have been confirmed from the relaxation strengths $\Delta\epsilon$ of the components which have been calculated by fitting the frequency dependence curves to the Havriliak−Negami (HN) equation.[59] The relaxation strengths for the fast and slow modes are proportional to the content of PBO and PVE, respectively, indicating that the fast and slow modes are due to PBO and PVE.

The Arrhenius plot of the loss maximum frequency f_{ms} for the fast mode and that f'_{ms} for the slow mode for 90/10 and 75/25 blends are shown in Figure 4. The separation $\log(f_{\mathrm{ms}}/f'_{\mathrm{ms}})$ of the fast and slow modes in the 90/10 blend is 3.5 decades at $1000/T = 3.7$. Thus, the segmental dynamics of the PBO chains is much faster than that of the PVE chains. We attempted to estimate the dielectric glass transition temperature T_D, which is defined as the temperature at which f_m becomes

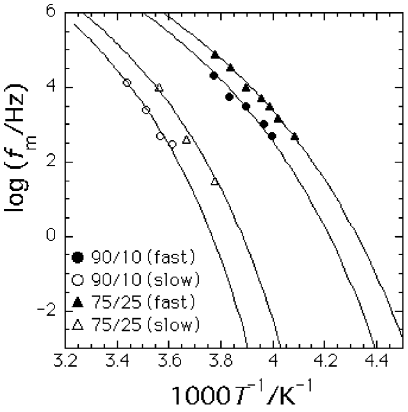

Figure 4. Arrhenius plots of the loss maximum frequencies f_m for the bimodal loss peaks of PVE-89/PBO-50 with compositions of 90/10 and 75/25.

Table 4. Dielectric Glass Transition Temperature T_D and the Effective Glass Transition Temperature T_{g-eff} of PVE/PBO Blends

composition	T_D	T'_D	T_{g-eff}(PBO)	T_{g-eff}(PVE)
90/10	228 ± 4	256 ± 4	221	258
75/25	221 ± 4	248 ± 4	216	247

10^{-3} Hz. As is well-known, T_g corresponds to the temperature at which the segmental relaxation time becomes the time scale of DSC measurements, namely 100 s ($f_m = 1/(2\pi\tau) \approx 10^{-3}$). We extrapolated the Arrhenius plots with the aid of the Vogel–Fulcher equation:[60,61]

$$\log f_m = A - \frac{B}{T - T_0} \tag{2}$$

where A, B, and T_0 are the parameters. Since data points are scattered in Figure 4, it is difficult to determine the reliable values of the parameters. Therefore, A and B are assumed to be equal to those for the fast mode of the PVE-31/PBO-20 blend (75/25) which will be described later (see Figure 6), i.e., $A = 11.9$ and $B = 566$ K. Only T_0 is assumed to be adjustable. Thus, estimated Arrhenius plots are represented by the solid lines in Figure 4. T_D for the fast mode and T'_D for the slow mode are listed in Table 4. T_D and T'_D correspond to the temperatures at which segmental motions of the PBO and PVE chains are frozen in. Although the PBO chains are mostly surrounded by the PVE chains in the 90/10 blend, the PBO chains move much faster than the PVE chains. In the range $T_D < T < T'_D$, the segmental motions of PBO are not frozen in, but the PVE chains are in the glassy state. Dynamics in such the nonequilibrium state has been reported for blends of poly(methyl methacrylate) (PMMA)/poly(ethylene oxide) (PEO)[21,23,39] and PS/PVME blends.[9,10,12,13]

Lodge and McLeish[53] explained the dynamic heterogeneity on the basis of the concept of self-concentration. The model assumes that the friction for the A chains in a miscible blend composed of A and B is determined by the local concentration ϕ in the local region of the cube of the Kuhn length l_K^3 surrounding the A-segment. The effective local concentration (volume fraction) ϕ_{eff} of the A-chains is given by

$$\phi_{eff} = \phi_s + (1 - \phi_s)\phi \tag{3}$$

where ϕ_s is the volume fraction of the A-chain in the volume of l_K^3 and ϕ is the average concentration of A. The value of ϕ_s for PVE is reported to be 0.25.[53] For PBO, the unperturbed dimension was reported by Matsushima et al.[62] From their data, the characteristic ratio C_∞ and l_K of the PBO chain are calculated to be 5.23 and 0.784 nm, respectively. Thus, ϕ_s of PBO becomes 0.44. It is noted that ϕ_s and T_g of *cis*-polyisoprene (PI) are 0.45 and 200 K, respectively. Therefore, the PVE/PBO system is similar to the PVE/PI system. For the PVE/PI system, it is difficult to observe the dynamics of PI in the PVE-rich region by the dielectric method, say $w_{PVE} > 0.5$. This disadvantage may be covered by PVE/PBO blends.

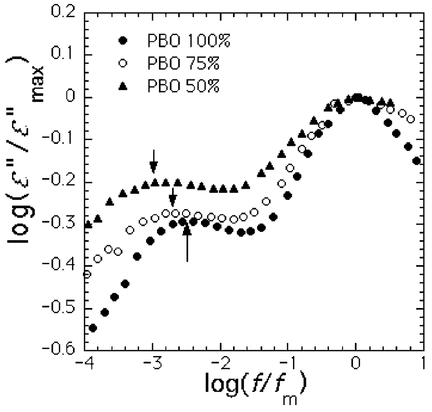

Figure 5. Normalized ϵ'' curves for PVE-89/PBO-4 blends. The arrows indicate the loss maximum frequencies of the normal mode of PBO-4 in the blends.

The effective glass transition temperatures T_{g-eff} at the PBO content of 0.1 and 0.25 have been determined and compared with the dielectric glass transition temperatures. The results are listed in Table 4. For 90/10 and 75/25 blends, the values of ϕ_{eff} have been calculated with eq 3, and then ϕ_{eff} is converted into the weight fraction. Thus, the values of T_{g-eff} at ϕ_{eff} were read from Figure 1. Here we assumed that the density of the blends was given by the weighted average of 0.89 g cm^{-3} for PVE[63] and 0.98 g cm^{-3} for PBO.[64] As is seen in Table 4, the Lodge–McLeish model explains fairly well the present experimental results. Lodge and McLeish[53] calculated T_{g-eff} using the Fox equation.[56] If the Fox equation is used to calculateT_{g-eff} without using the experimental data given in Figure 1, the calculated values of T_{g-eff} agree well with T_D and T'_D within ±1 K.

Relationship between Normal and Segmental Modes in PVE/PBO Blends. Since the dielectric response of PBO is dominant in PVE/PBO blends with $w_{PBO} > 0.25$, we can examine the effect of blending on the relationship between the relaxation time of the normal mode τ_n and that of segmental mode τ_s for the one component namely PBO. The dynamical behavior of PVE is invisible.

Figure 5 shows the ϵ'' curves of PVE-89/PBO-4 blends. The curves are normalized by the maximum value ϵ''_{max} and loss-maximum frequency f_{ms} for the segmental mode. As indicated by the arrows, the separation $\log(f_{ms}/f_{mn})$ of the loss-maximum frequencies between the segmental and normal modes increases with increasing PVE content. The difference of $\log(f_{ms}/f_{mn})$ between pure PBO-4 and the 50/50 blend is 0.50 decade.

A similar test was also made for PVE-31/PBO-20 blends. In those blends the value of $\log(f_{ms}/f_{mn})$ becomes wider than our experimental window, and hence $\log(f_{ms}/f_{mn})$ has been determined by extrapolation of the Arrhenius plot (Figure 6).

The solid lines in Figure 6 show the fitting curves to the VF equation. First, the parameters A, B, and T_0 for the segmental modes were determined as listed in Table 5. Second, the parameters B and T_0 for the normal mode were assumed to be the same as those of the segmental modes, and only A was assumed to be adjustable. Thus, the solid lines for the normal and segmental modes for each composition change keeping $\log(f_{ms}/f_{mn})$ constant. To minimize the error due to extrapolation, the values of $\log(f_{ms}/f_{mn})$ have been determined at 256 K, which

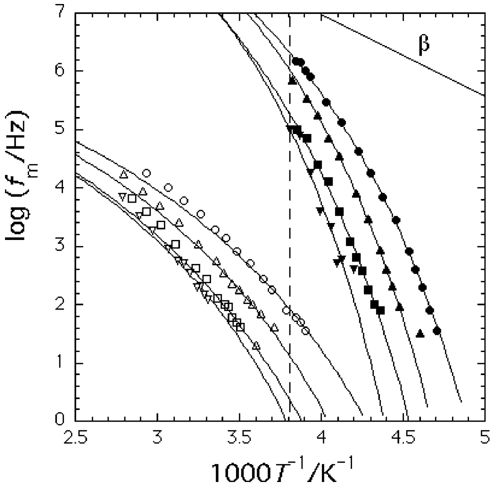

Figure 6. Arrhenius plots of the loss maximum frequencies f_m for the segmental mode (closed keys) and the normal modes (open keys) for PVE-31/PBO-20. The compositions (w/w): circle, 0/100; triangle, 25/75; quadrangle, 50/50; and inverted triangle, 75/25. The solid curved lines represent the Vogel−Fulcher equation (Table 5). The straight line indicates the Arrhenius plot for the β process of the 50/50 blend.

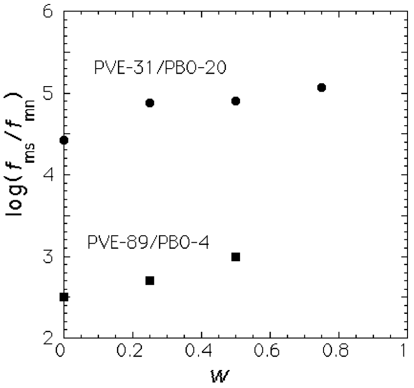

Figure 7. Composition dependences of the separation of log f_{ms} and log f_{mn} in PVE/PBO blends. w denotes the weight fraction of PVE.

Table 5. Dependence of Parameters of the Vogel−Fulcher Equation on Weight Fraction w of PBO for PVE-31/PBO-20

	segmental mode			normal mode		
w	A	B	T_0	A	B	T_0
1	11.4	531	158.2	7.0	531	158.2
0.75	11.9	566	180.6	6.8	566	180.6
0.50	11.9	635	167.0	7.0	635	167.0
0.25	11.9	566	166.5	7.0	566	166.5

corresponds to $1000/T = 3.8$ (dashed line in Figure 6). In Figure 6 we notice that the Arrhenius plots for the normal modes in the range of $2.8 < 1000/T < 3.2$ deviate slightly upward from the VF equation. Therefore, log(f_{ms}/f_{mn}) depends slightly on temperature.

The Arrhenius plot for the β processes of the PVE/PBO (50/50) blend is shown in Figure 6. In our previous paper on the dielectric relaxation of pure polyethers,[47] we found that the α and β relaxations of PiPGE and PtBGE merge at about 10^6 Hz. The β relaxation in the present blend occurs at much higher frequencies than the segmental relaxation, and hence the β process in PVE/PBO blends does not affect much the segmental dynamics. As will be shown later, similar behavior was observed for the β process in blends of PiPGE/PtBGE and PnBGE/PtBGE (see Figures 19 and 20).

Thus, determined values of log(f_{ms}/f_{mn}) are plotted in Figure 7 together with the results for PVE-89/PBO-4. We see that log(f_{ms}/f_{mn}) increases slightly with increasing PVE content. The difference of log(f_{ms}/f_{mn}) between pure PBO and the 50/50 blend is 0.5 decade. It is stressed that f_{ms} and f_{mn} change several decades with temperature and composition, but the temperature and composition dependences of log(f_{ms}/f_{mn}) are very weak.

The relationship between the terminal chain dynamics and local segmental motions was investigated by Verdier and Stockmayer, who performed a computer simulation for a chain consisting of N beads placed on the lattice points of a cubic lattice.[65] Each bead jumps randomly to one of the neighboring lattice points. The successive occurrence of random local jumps of the beads results in fluctuation of the end-to-end distance. They found that although the model is quite different from the bead−spring model, the terminal relaxation time τ_1 is proportional to N^2 conforming to the Rouse theory:[66]

$$\tau_1 = K(N-1)^2\tau_0 \tag{4}$$

where K is the constant close to unity and τ_0 is the correlation time for local jump of the beads. Since $N \gg 1$, τ_1 is proportional to $N^2\tau_0$. It is reasonable to consider that one bead of the theory corresponds to average unit of segmental dynamics consisting of several monomer units and that the experimentally observed τ_n ($=1/(2\pi f_{mn})$) and τ_s ($=1/(2\pi f_{ms})$) correspond to τ_1 and τ_0, respectively. This equation explains well the present experimental results, i.e., although τ_0 changes rapidly with temperature and composition, f_{ms}/f_{mn} remains almost constant. The dielectric data for PI/PVE blends indicate that f_{ms}/f_{mn} for PI is almost independent of composition, and therefore the result can be also explained by eq 4. We expect that the size of the segment changes with composition depending on the intermolecular interactions between the components. In such a case, N depends on the composition and hence f_{ms}/f_{mn} depends on the composition.

The Verdier−Stockmayer approach may work for the case where the differences between the composition and temperature dependence of the segmental and normal-mode frequencies are apparently small. Several cases where f_{ms}/f_{mn} depends strongly on the composition have been reported.[37−40] Lutz et al.[21] and Haley and Lodge[39] found that the PEO segmental dynamics are almost composition independent, whereas the terminal dynamics are dramatically reduced by the presence of PMMA. He et al. observed the strong composition dependence of $\zeta/\tau_s T$ in PI/PS and polybutadiene/PVE blends where ζ is the friction coefficient for the terminal chain dynamics.[22,24] Thus, there are two groups of blends: one is blends in which the composition and temperature dependence of f_{ms}/f_{mn} is weak, and the other is those exhibiting a strong dependence. We notice a strange coincidence that in the former the segmental dynamics was measured by dielectric spectroscopy, but in the latter NMR was used. This difference in the technique of measurements might be the origin of difference of the two groups. We speculate that the length scale of the segmental dynamics detected by NMR is shorter than that detected by the dielectric method.

Broadening of Relaxation Spectra of PBO in PVE/PBO Blends. Parts a and b of Figure 8 show the normalized ϵ'' curves for the segmental and normal modes of the PBO chains in blends of PVE-31/PBO-20, respectively. It is seen in Figure 8a that the ϵ'' curve for the segmental mode broadens markedly with increasing PVE content, while that of the normal mode broadens little. Since the observed ϵ'' is due to only PBO, the results cannot be explained in terms of the distinct segmental dynamics as proposed by the Lodge−McLeish model (eq 3).[53] The present result indicates that the distribution of segmental relaxation times for one component broadens in blends due to local concentration

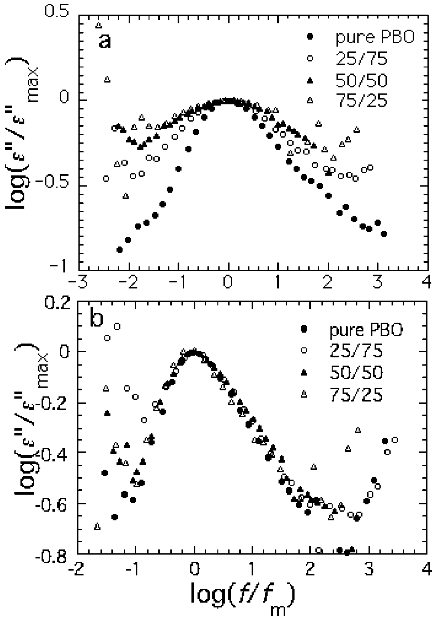

Figure 8. Normalized ϵ'' curves for (a) the segmental mode and (b) the normal mode of PVE-31/PBO-20 blends.

fluctuation. Zetsche and Fischer[51] analyzed the dynamic behaviors of blends assuming a Gaussian distribution of local concentration. The results shown in Figure 8a,b indicate that the correlation length ξ of concentration fluctuation is longer than the relevant length of segmental motions but shorter than the end-to-end distance of PBO-20 ($\langle r^2\rangle^{1/2} = 3.14$ nm).[62] Similar behavior was observed for PI/PVE blends.[14] Here it is interesting to examine the ϵ'' curve of PVE-89/PBO-4 in which the end-to-end distance of PBO-4 is 1.42 nm. In Figure 5 we see that the ϵ'' curve for the normal mode of PBO-4 broadens with increasing PVE content, in contrast to PBO-20. However, the extent of broadening is not so large compared with the segmental mode, and hence $\langle r^2\rangle^{1/2}$ of the PBO-4 chains is close to ξ but slightly longer than ξ. It is reminded that the Kuhn length of PBO is 0.78 nm, which is assumed to be the size of segmental motions in the Lodge−McLeish model.[53] From those data, ξ in PVE/PBO blends is estimated to be 1.0 ± 0.3 nm. A similar value of the relevant length of the segmental dynamics was obtained for PI/PB blends.[14] Since both of the bimodal behavior and the broadening of the ϵ'' curve of the component have been observed, the present results indicate that the dynamic heterogeneity arises at least from two origins namely the difference of intrinsic mobility of the components and concentration fluctuation.

2. Dielectric Relaxation in Blends of Polyethers. In the previous section the bimodal segmental mode has been observed for PVE/PBO with the content of PBO less than 25 wt %. In PVE/PBO, ΔT_g of the components is 70 K, and the intensity of PBO is much higher than that of PVE. In this section we examine the behavior of blends in which ΔT_g is less than 70 K, but the components exhibit similar dielectric intensity. The high-T_g component is PtBGE-37, and the low-T_g component is PBO-12, PiPGE-22, or PnBGE-25. Among these polyethers, T_g of PtBGE is the highest (249 K) and that of PnBGE(194K) is the lowest. Thus, the effect of ΔT_g ranging from 55 to 43 K on the dynamic heterogeneity has been investigated.

PBO-12/PtBGE-37. Figure 9 shows the temperature dependences of ϵ'' at 1 and 10 kHz for the PBO-12/PtBGE−37 (50/50) blend. Unfortunately, the ionic conductivity was high as shown for the ϵ'' vs T curve at 1 kHz, and hence the correction of the ionic conduction was made. After the correction, the loss peak due to the normal mode of PBO-12 [α_n(PBO)] is observed around 270 K. The main peak is due to the segmental mode (α_s) due to local segmental motions of PBO-12 and PtBGE-37. In contrast to the PVE/PBO blends the α_s loss peak is unimodal at all composition. The β relaxation occurs around 150 K. Since MW of PtBGE-37 is higher than that of PBO-12, the normal mode relaxation of PtBGE-37 is expected to occur above 310 K at 1 kHz from the dielectric data of pure PtBGE-37 reported previously.[47] Unfortunately, the ionic conductivity was too high to detect the normal mode of PtBGE-37.

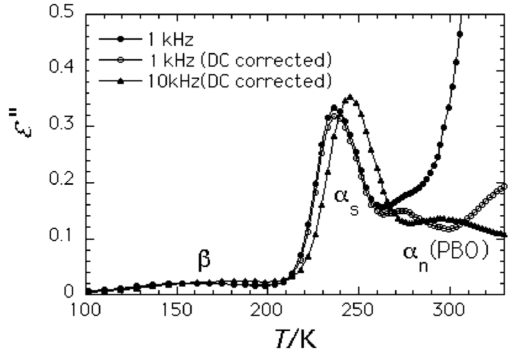

Figure 9. Temperature dependence of ϵ'' for PBO-12/PtBGE-37 (50/50).

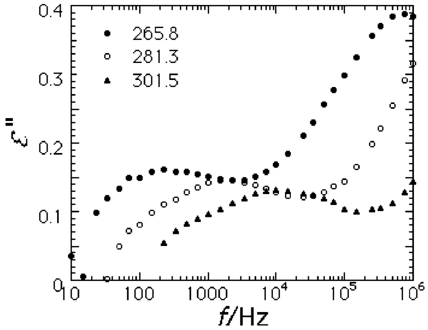

Figure 10. Frequency dependence of ϵ'' for PBO-12/PtBGE (50/50).

Figure 10 shows the frequency dependence of ϵ'' for PBO-12/PtBGE-37. The low-frequency peaks are the normal mode of PBO-12, and the increase of ϵ'' with increasing frequency is due to the segmental modes of PBO and PtBGE. Similar $\epsilon''-f$ curves were observed for the 75/25 blend. The normal mode of the 25/75 blend was very weak due to low content of PBO, and the reliable loss curve was not obtained for this blend. The normal mode relaxation of PtBGE-37 is expected to occur around 1 Hz at 265.8 K but was not observed clearly at all compositions due to the ionic conduction.

Figure 11 compares the ϵ'' curves for the normalized $\epsilon''-f$ curves for the segmental mode of PBO-12/PtBGE-37. As mentioned above, the segmental mode is unimodal. We see that the ϵ'' curve of the 75/25 blend is broad in the low-frequency side, but conversely, the ϵ'' curve of the 25/75 blend is broad in the high-frequency side. The ϵ'' curve of the 50/50 blend is broad and almost symmetrical. These behaviors suggest that the relaxation spectra of the blends consist of two relaxation regions with intensities proportional to the contents of the components. In other words, the ϵ'' curves due to PBO and PtBGE locate respectively at slightly higher and lower frequencies than the loss-maximum frequency F_{ms} of the blends. Since the relaxation times of the components are close, the ϵ'' curves become apparently unimodal.

From those results for blends of PBO/PtBGE, the $\epsilon''-f$ curve of a miscible blend composed of type AB polymers I and II is schematically drawn as shown in Figure 12. Here we consider

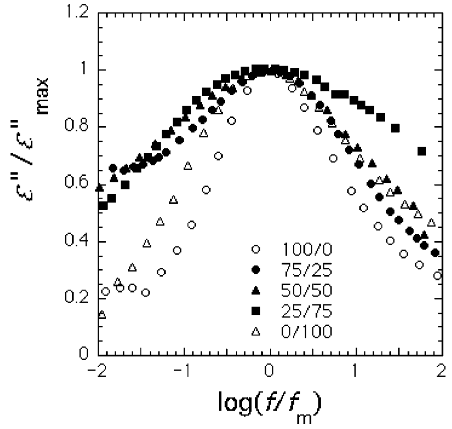

Figure 11. Normalized ϵ'' curves for the segmental mode of PBO-12/PtBGE-37. Compositions are indicated in the figure.

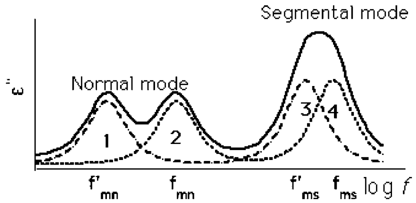

Figure 12. Schematic representation of the $\epsilon''-f$ curve of a 50/50 blend composed of polymers I and II which exhibit both the segmental and normal modes.

the case that I and II are low- and high-T_g components, respectively, and the composition is 50/50. The loss peaks 1 and 3 are due to the normal and segmental modes of the component I, and the peaks 2 and 4 are due to the component II in the blend. On account of the distinct segmental dynamics of I and II, the locations of the loss peaks 3 and 4 are different. The separations between the peaks 1 and 3 or between the peaks 2 and 4 are determined fundamentally by the molecular weights of the components: the M dependence of the separation is governed by either the Rouse theory[66] or the 3.4 power law depending on the characteristic molecular weight.[58] The data of PVE/PBO in which only peaks 2 and 4 are observable indicate that the separation increases by δ (= ca. 0.5 decades at 50/50 composition) with increasing content of PVE (see Figure 7). We denote the loss-maximum frequencies for the peaks 1, 2, 3, and 4 as f'_{mn}, f_{mn}, f'_{ms}, and f_{ms}, respectively. We also denote the loss-maximum frequency for the segmental mode of the blend as F_{ms}.

Returning to the dielectric data of PBO/PtBGE, we attempt to estimate the location of the PBO peak in the $\epsilon''-f$ curve of the 50/50 blend. We assume that the separation of the segmental and normal modes $\log(f_{ms}/f_{mn})$ of PBO-12 in the 50/50 blend (Figure 10) is 0.5 decade wider than that in the pure state. It is noted that $\log(f_{ms}/f_{mn})$ in PI/PVE blends is almost independent of composition.[14] However, this assumption is not harmony with the results reported in refs 37−40. Thus, the assumption used in the following discussion is a tentative working hypothesis.

Figure 13 shows the comparison of the $\epsilon''-f$ curves between PBO-12/PtBGE-37(50/50) and pure PBO-12. The ϵ'' curve of pure PBO has been shifted so that the peaks for the normal modes of the blend and pure PBO coincide. As is seen in this figure, the separation of the segmental and normal modes of pure PBO provides a measure to estimate the peak position f_{ms} of the segmental mode of PBO in the blend. Here we have assumed that the separation of the segmental and normal modes of PBO in the blend is wider than that of pure PBO by δ (=0.5) decade. For the sake of later discussion, the difference of the peak frequencies for the segmental mode for the blend and pure PBO is denoted as Δ, as shown in Figure 13. The present result indicates that the components move at different rates even though the loss curve of the blend is unimodal. Only when ΔT_g of the components is large, the bimodal loss curve is dielectrically observed.

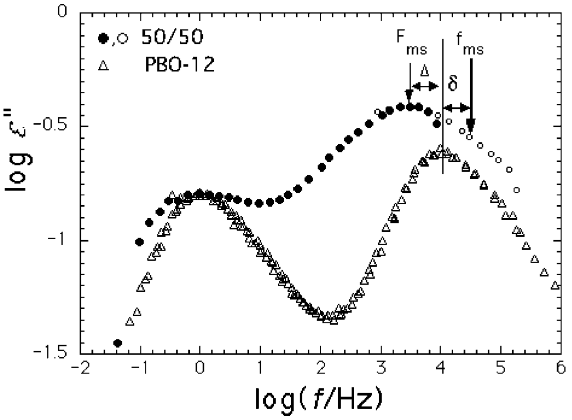

Figure 13. Comparison of the frequency dependences of ϵ'' between PBO-12/PtBGE-37 (50/50) and pure PBO-12. The curves are shifted so that the peaks for the normal modes coincide. The solid line indicates the loss maximum frequencies of the segmental mode of pure PBO. The arrows indicate F_{ms} and the estimated f_{ms} of PBO-12 (fast mode) in the 50/50 blend.

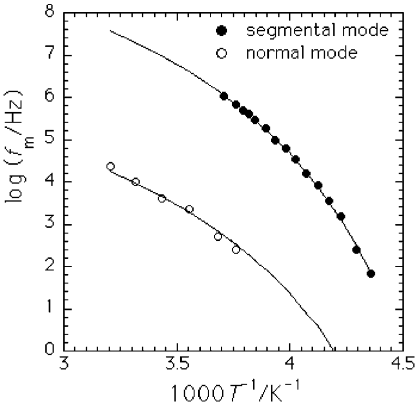

Figure 14. Arrhenius plots of F_{ms} and f_{mn} for PBO-12/PtBGE-37 (50/50).

Figure 14 shows the Arrhenius plots of the loss-maximum frequencies for the 50/50 blend. It is noted that the Arrhenius plots for the segmental mode of PVE/PBO (Figure 6) and those for PBO/PtBGE (Figure 12) have different physical meanings: in the former f_{ms} for the fast mode is plotted but in the latter F_{ms}, which is a weighted average of f_{ms} and f'_{ms}. On the other hand, f_{mn} for the normal mode is due to only the PBO-12 chains in the blend (see Figure 12). The plots of F_{ms} have been fitted to the VF equation with $A = 10.5$, $B = 367$, and $T_0 = 187.3$ as represented by the solid line. For f_{mn} we have used the same values of B and T_0 as those for F_{ms}, and only A (=7.2) has been changed. Thus, the solid lines in Figure 14 change keeping $\log(f_{ms}/f_{mn})$ constant with temperature. We see that the data points locate close to these lines. Since the VF equation conform well to the Arrhenius plots for the segmental mode, extrapolation on the basis of the VF equation is reliable. This behavior is similar to that of homopolymers; i.e., f_{ms}/f_{mn} is independent of temperature in the range $T > T_g + 30$ K.[44,45] We conclude that in the range of audio frequency the separation between the normal mode of the component and the average of the segmental relaxation frequencies does not change appreciably with temperature.

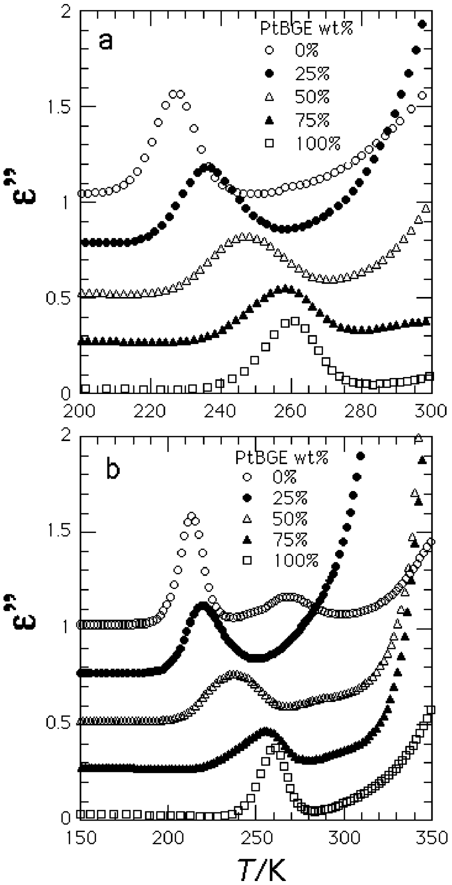

Figure 15. Temperature dependences of ϵ'' for (a) PiPGE-22/PtBGE-37 and (b) PnBGE-25/PtBGE-37 blends at 1 kHz. The baselines are shifted upward by 1, 0.75, 0.5, and 0.25 for the ϵ'' curves of the blends with PtBGE contents of 0, 25, 50, and 75 wt %, respectively.

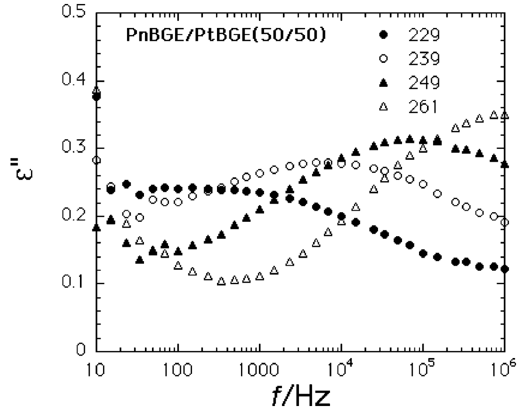

Figure 16. Frequency dependence of ϵ'' of PnBGE-25/PtBGE-37 (50/50) in the temperature region where the segmental mode is observed. Temperatures are given in the figure.

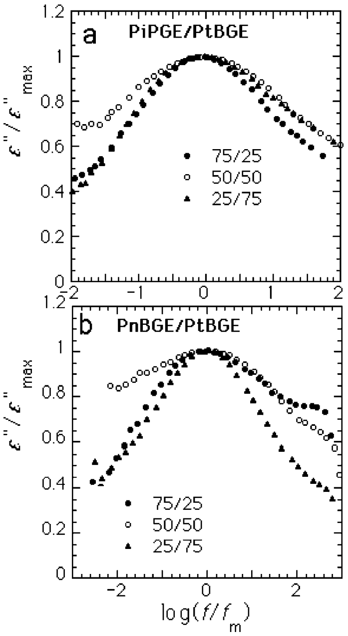

Figure 17. Normalized ϵ'' curves for the segmental mode of (a) PiPGE-22/PtBGE-37 and (b) PnBGE-25/PtBGE-37. Compositions are indicated in the figure.

Blends of PiPGE/PtBGE and PnBGE/PtBGE. Figure 15 shows the $\epsilon''-T$ curves for blends of PiPGE-22/PtBGE-37 and PnBGE-25/PtBGE-37. Both blends exhibit unimodal ϵ'' peaks for the segmental mode at all compositions. Comparing these blends, we see that the composition dependences of the $\epsilon''-T$ curves for the segmental modes are similar; i.e., the $\epsilon''-T$ curves for the blends with 75/25 and 25/75 compositions are broad in the high-temperature side and low-temperature side, respectively. Especially the $\epsilon''-T$ curves of the blends with 25/75 composition exhibit the asymmetrical shapes. Since the dipole moments of the components are similar,[47] the behaviors seen in Figure 15 indicate the distinct segmental dynamics of the components as observed for PBO/PtBGE blends.

So far we have discussed the composition dependence of the ϵ'' curves for the segmental mode of blends. Here we examine the temperature dependence of the segmental mode. Figure 16 shows the representative ϵ'' curves for PnBGE-25/PtBGE-37 (50/50) in the temperature region of the segmental mode. It is seen that the ϵ'' curve broadens with decreasing temperature. This behavior was observed for all blends examined in this study. One may attribute this behavior to the distinct temperature dependences of the fast and slow modes: the temperature dependence of the slow mode is stronger than the fast mode. However, this view may be ruled out because even in the case where only the fast mode is observable, the loss curve broadens much with decreasing temperature, as shown in Figure 8a. Similar behavior is seen in blends of poly(vinyl methyl ether) (PVME)/PS, in which PS is dielectrically almost inactive, but the dielectric loss curves of PS/PVME blends broaden much with decreasing temperature.[9] Therefore, the temperature dependence of the width of the loss curve for the segmental mode is due to concentration fluctuation although the broadening is due to both the distinct mobilities of the components and concentration fluctuation. We consider that the ratio of f_m for the fast and slow modes is almost independent of temperature. For concentrated toluene solutions of poly(vinyl acetate), we found that the half-width of the loss curve of the segmental mode is proportional to $(T - T_0)^{-2}$, where T_0 is the Vogel temperature.[67] This dependence can be derived by assuming a Gaussian distribution of local concentration.[67]

Parts a and b of Figure 17 show the normalized $\epsilon''-f$ curves for PiPGE-22/PtBGE-37 and PnBGE-25/PtBGE-37 blends, respectively. The ϵ'' curves which exhibit maxima at about 1 kHz have been used for this comparison. Although ϵ'' curves broaden with decreasing temperature, the asymmetrical shapes are almost independent of temperature. The composition dependences of the shapes of the $\epsilon''-f$ curves are similar to the PBO/PtBGE blends (Figure 11), indicating that those ϵ'' curves are also composed of the fast and slow modes although the loss curves are unimodal. It is noted that the ordinary ϵ'' curve is expressed by the Havliriak−Negami equation[59] and is normally broad in the high-frequency side. If this is taken into account,

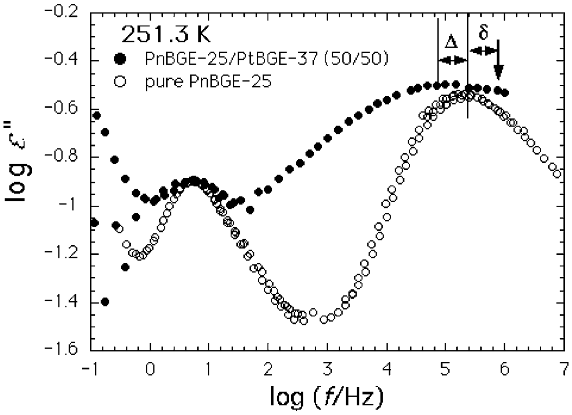

Figure 18. Comparison of the ϵ'' curves of pure PnBGE-25 and the blend of PnBGE-25/PtBGE-37 with the composition of 50/50 (w/w).

we consider that the almost symmetrical ϵ'' curve seen in Figure 17 has a broader distribution of relaxation times in the low-frequency side.

Estimation of Relaxation Frequency of Low-T_g Component. On the basis of the same procedure as applied to the PBO/PtBGE blends, the $\epsilon''-f$ curve of PnBGE-25/PtBGE-37 (50/50) has been analyzed. Figure 18 shows comparison of the ϵ'' curves between pure PnBGE-25 and the blend of PnBGE-25/PtBGE-37 (50/50). The master curve of ϵ'' has been used for the blend to extend the frequency range. Usually the time–temperature superposition (tTS) is not applicable to blends.[6] However, as seen in Figure 8b and also known for the PI/PVE blend,[14] the tTS principle holds for the normal mode if the MW is high. Therefore, tTS has been applied only in the normal mode region. Separation of the normal and segmental modes of the blend has been determined by extrapolation of the Arrhenius plot for the normal mode (Figure 20). In Figure 18 the ϵ'' curve for pure PnBGE is shifted so that the peaks for the normal modes of PnBGE and the blend coincide. We again define the separations Δ and δ as shown in Figure 18 as defined for the PBO/PtBGE blend (see Figure 13). Thus, we estimate that f_{ms} of the PnBGE chains locates around $\log f = 5.9$, as indicated by the arrow. Here we have assumed that $\delta = 0.5$ decade.

To determine the separation of the normal and segmental modes, the Arrhenius plots are needed as mentioned above. Figures 19 and 20 show the Arrhenius plots of loss maximum frequencies F_{ms} (filled keys) and f_{mn} (open keys) of the low-T_g component for blends of PiPGE-22/PtBGE-37 and PnBGE-25/PtBGE-37, respectively. At 25/75 composition, the intensity of the normal mode was too weak to determine f_{mn}, and therefore only the values of F_{ms} have been plotted. From these plots the separation $\log(F_{ms}/f_{mn})$ between the segmental and normal modes has been determined by extrapolating the plots. For this purpose we fitted the plots to the VF equation (eq 2), and the parameters of the VF equation are listed in Table 6. To minimize the error of extrapolation of the Arrhenius plots, $\log(F_{ms}/f_{mn})$ has been determined at a temperature at which the extrapolations for both of the normal and segmental modes become minimum. For example, $\log(F_{ms}/f_{mn})$ of PnBGE-25/PtBGE-37 (50/50) has been determined at $10^3/T = 3.8$.

Figure 21 shows the composition dependence of $\log(F_{ms}/f_{mn})$. The value of F_{ms} at 75/25 composition is given approximately by the weighted average of 3:1 of the contributions of the low-T_g and high-T_g components. Thus, $\log(F_{ms}/f_{mn})$ for the 75/25 blends is intermediate of $\log(f_{ms}/f_{mn})$ of the pure low-T_g component and $\log(F_{ms}/f_{mn})$ of the 50/50 blends.

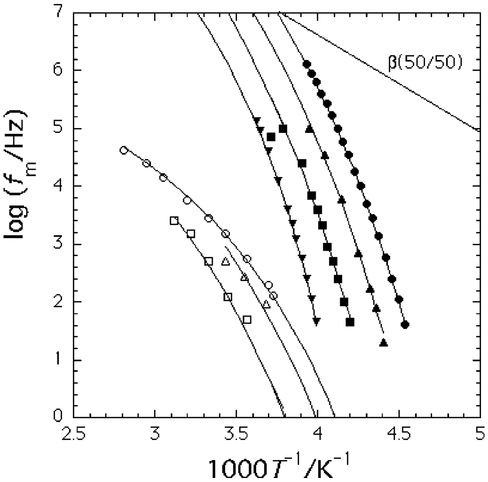

Figure 19. Arrhenius plots for PiPGE-22/PtBGE-37 blends. The solid and open keys indicate the segmental mode (F_{ms}) of the blend and the normal mode (f_{mn}) of PiPGE, respectively. The compositions (w/w): circle, 100/0; triangle, 75/25; quadrangle, 50/50; and inverted triangle, 25/75. The curved lines represent the Vogel–Fulcher equation (Table 6). The straight line indicates the loss maximum frequency for the β process of the blend with 50/50 composition.

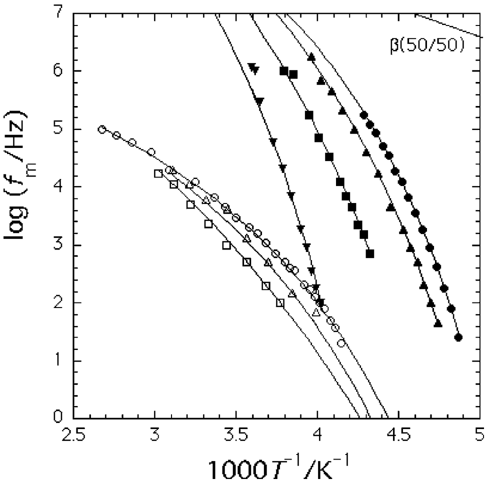

Figure 20. Arrhenius plots for PnBGE-25/PtBGE-37 blends. The solid and open keys indicate F_{ms} of the blends and f_{mn} of PnBGE in the blends, respectively. The compositions (w/w): circle, 100/0; triangle, 75/25; quadrangle, 50/50; and inverted triangle, 25/75. The solid lines represent the Vogel–Fulcher equation (Table 6). The straight line indicates the loss maximum frequency for the β process of the blend with 50/50 composition.

Table 6. Parameters of the Vogel–Fulcher Equation for PiPGE-22/PtBGE-37 (PiP) and PnBGE-25/PtBGE-37(PnB)[a]

		segmental			normal mode		
code	w	A	B	T_0	A	B	T_0
PiP	1	13.9	729	161.0	7.2	455	181.0
PiP	0.75	13.9	781	164.4	9.1	781	164.4
PiP	0.50	13.9	827	170.3	9.0	827	170.3
PiP	0.25	11.6	484	201.8			
PnB	1	11.2	421	162.0	7.2	458	162.0
PnB	0.75	12.1	562	157.1	7.6	562	157.1
PnB	0.50	13.3	769	157.6	9.3	1049	122.0
PnB	0.25	13.2	677	188.0			

[a] w denotes weight fraction of either PiPGE or PnBGE.

Dynamic Heterogeneity. In this final section we aim to estimate the magnitude of dynamic heterogeneity defined by $\log(f_{ms}/f'_{ms})$ for the 50/50 blends where f_{ms} and f'_{ms} are the loss-maximum frequencies of the peak 4 and peak 3 in Figure 12, respectively. Since the loss peak f'_{mn} for the normal mode

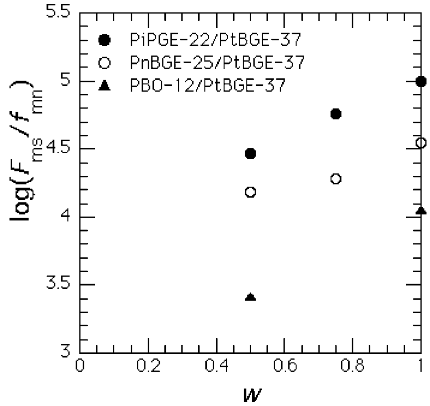

Figure 21. Dependence of log(F_{ms}/f_{mn}) on the weight fraction *w* of the low-T_g component in blends of PiPGE-22/PtBGE-37 and PnBGE-25/PtBGE-37.

of PtBGE-37 could not be observed for blends, we have estimated f'_{ms} of the PtBGE-37 chains in the blend as follows. As shown in Figures 13 and 18, log f_{ms} for the low-T_g component is equal to log $F_{ms} + \Delta + \delta$. A similar definition for the high-T_g component is written as log f'_{ms} = log $F_{ms} + \Delta' + \delta'$. As mentioned above, information on Δ' and δ' is not available.

It is expected that Δ' is negative and approximately equal to $-\Delta$ since we are considering the symmetrical 50/50 blend. From the shape of the ϵ'' curves this is rationalized. What is the value of δ'? It is known that δ' becomes negative when a diluent (low-T_g component) is added to a polymer (high-T_g component) for the polyisoprene/toluene system.[68] Therefore, we expect that δ' in the blends of polyethers is also negative.

This can be explained by the Verdier–Stockmayer model (eq 4) which predicts that the value of log(f_{ms}/f_{mn}) depends on the relevant size of segmental dynamics. When a polymer chain is surrounded by a low-T_g component, segmental motions of a larger size are allowed, and hence the relevant size increases, resulting in a negative δ'. Contrary, when a low-T_g component is surrounded by high-T_g polymer chains, the reverse shift occurs resulting in the positive δ.

From those considerations we estimate roughly the values of log(f_{ms}/f'_{ms}) to be $2\Delta <$ log(f_{ms}/f'_{ms}) $< 2\Delta + 2\delta$. For the upper and lower bounds, we have assumed that $\delta' = -\delta$ and $\delta' = \delta$, respectively. The other method for estimation of log(f_{ms}/f'_{ms}) is the curve fitting. We have obtained a result that log(f_{ms}/f'_{ms}) is close to $2(\Delta + \delta)$ for the blends of PBO/PtBGE, PiPGE/PtBGE, and PnBGE/PtBGE.[69]

Figure 22 shows the plots of log(f_{ms}/f'_{ms}) vs ΔT_g for blends of polyethers examined in this study and those reported so far.[10,13,14] The data points in the range $\Delta T_g > 70$ are those for blends which exhibit bimodal ϵ'' curve, and the values of log(f_{ms}/f'_{ms}) are read directly from the ϵ'' curves. It is seen that log(f_{ms}/f'_{ms}) is approximately proportional to ΔT_g but scatters appreciably from linearity. This is considered to be due to the different kind of intermolecular interactions between the components. In the blends of PVE/PI and PVME/PS[10] only van der Waals interactions prevail, but in P2CS/PVME[13] and polyethers/PtBGE blends the dipole–dipole interactions act as well as van der Waals interactions. In those plots systematic deviation of the latter from the former is not seen. Therefore, the dipole–dipole interactions do not affect strongly the dynamic heterogeneity. However, Zhang et al.[30,31] reported that miscible polymer blends in which intermolecular hydrogen bonds are formed exhibit unimodal ϵ'' curves for the segmental mode despite large ΔT_g. Thus, the intermolecular interactions are important factor for dynamic heterogeneity.

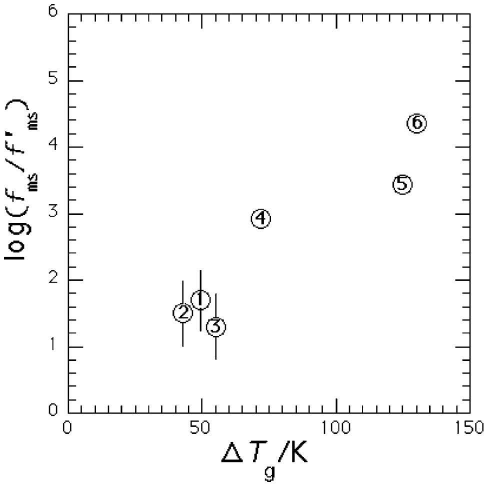

Figure 22. Dependence of the separation of the segmental relaxation frequencies log(f_{ms}/f'_{ms}) of the components in miscible blends with 50/50 composition (see Figure 12) on the difference ΔT_g of glass transition temperatures of the components. 1, PBO-12/PtBGE-37; 2, APiPGE-22/PtBGE-37; 3, BPnBGE-25/PtBGE-37; 4, CPI/PVE;[7,14] 5, DPVME/PS;[10] 6, EPVME/P2CS.[13] For the plots 4–6, the separation has been determined at $T = T_g + 30$ K. The error bars for the plots 1–3 indicate the upper and lower bounds in estimation of the separation (see text).

Conclusion

Dynamic heterogeneity in blends of PVE/poly(butylene oxide) (PBO), PBO/poly(*tert*-butyl glycidyl ether) (PtBGE), poly(isopropyl glycidyl ether) (PiPGE)/PtBGE, and poly(*n*-butyl glycidyl ether) (PnBGE)/PtBGE has been investigated by means of dielectric relaxation spectroscopy. Dielectric data of those miscible blends provide us new information on the dynamic heterogeneity of segmental dynamics and the relationship between local segmental dynamics and terminal chain dynamics. In PVE/PBO blends, bimodal ϵ'' curves for the segmental mode have been observed. The fast and slow modes can be assigned to PBO and PVE, respectively. The separation log(f_{ms}/f'_{ms}) of the fast and slow modes in the 90/10 blend is determined to be 3.5 decades. The dielectric glass transition temperatures T_D for the fast mode and T'_D for the slow mode of the 90/10 and 75/25 blends agree fairly well with the effective glass transition temperatures $T_{g-\mathrm{eff}}$ proposed by Lodge and McLeish. Since the intensity of PBO is much higher than that of PVE, the dielectric data are due to PBO in the blends. Thus, in the range of the PBO content higher than 25 wt %, the composition dependences of the loss-maximum frequency for the segmental mode f_{ms} and that for the normal mode f_{mn} of PBO have been investigated. It is found that the separation log(f_{ms}/f_{mn}) for the 50/50 blend is wider than that of pure PBO by 0.5 decade. The ϵ'' curve for the segmental mode broadens markedly with decreasing temperature, while that of the normal mode broadens little. This result can be ascribed to local concentration fluctuation. The correlation length ξ of concentration fluctuation is estimated to be 1.0 ± 0.3 nm. From these results we conclude that the dynamic heterogeneity is due to both the distinct segmental dynamics of the components and concentration fluctuation.

The blends of polyethers, i.e., PBO-12/PtBGE-37, PiPGE-22/PtBGE-37, and PnBGE-25/PtBGE-37 exhibit unimodal ϵ'' curves for the segmental mode. In these blends, PBO, PiPGE, and PnBGE are the low-T_g component (I) and PtBGE is the high-T_g component (II). The dielectric intensities of components I and II are similar, and the differences of the glass transition temperatures ΔT_g between I and II are less than 55 K. The ϵ'' curves of the blends with the composition of I/II = 75/25 are broad in the low-frequency side. Conversely, the ϵ'' curves of the blends with I/II = 25/75 are broad in the high-frequency side, indicating that the loss maximum frequency f_{ms} due to I and that f'_{ms} due to II locate respectively at slightly higher and lower frequencies than the loss-maximum frequency F_{ms} of the blends. To estimate $\log(f_{ms}/f'_{ms})$ for the 50/50 blends, the separation between the normal and segmental modes $\log(f_{ms}/f_{mn})$ for I is assumed to increase by δ (=0.5 decade) by blending on the basis of the data for the blends of PBO/PVE. On the basis of this assumption, $\log f_{ms}$ is given by $\log F_{ms} + \Delta + \delta$, where Δ is the difference of $\log(F_{ms}/f_{mn})$ between pure low-T_g component and the 50/50 blend. Thus, we estimate roughly the values of $\log(f_{ms}/f'_{ms})$ with $2\Delta < \log(f_{ms}/f'_{ms}) < 2\Delta + 2\delta$. The values of $\log(f_{ms}/f'_{ms})$ for blends of polyethers examined in this study and those reported previously are approximately proportional to ΔT_g.

The analyses have been made on the basis of several assumptions which are not in harmony with the observations for the other blend systems. However, we see that the present procedure works well for three blends, i.e., PBO/PtBGE, PiPGE/PtBGE, and PnBGE/PtBGE, resulting in a reasonable ΔT_g dependence of the dynamic heterogeneity as shown in Figure 22. Therefore, we believe that the procedure used here is useful for blends in which there are no specific interactions. The present study has raised several issues which will be resolved by careful studies in the future.

References and Notes

(1) Olabisi, O.; Robeson, L. M.; Shaw, M. T. *Polymer−Polymer Miscibility*; Academic: New York, 1979.
(2) Utracki, L. A. *Polymer Alloys and Blends-Thermodynamics and Rheology*; Hanser Publishers: New York, 1990.
(3) Zetsche, A.; Kremer, F.; Jung, W.; Schulze, H. *Polymer* **1990**, *31*, 1883.
(4) Miller, J. B.; McGrath, K. J.; Roland, C. M.; Trask, C. A.; Garroway, A. N. *Macromolecules* **1990**, *23*, 4543.
(5) Katana, G.; Fischer, E. W.; Hack, T.; Avetz, V.; Kremer, F. *Macromolecules* **1995**, *28*, 2714.
(6) Colby, R. H. *Polymer* **1989**, *30*, 1275.
(7) Alegria, A.; Colmenero, J.; Ngai, K. L.; Roland, C. M. *Macromolecules* **1994**, *27*, 4486.
(8) Alvarez, F.; Alegria, A.; Colmenero, J. *Macromolecules* **1997**, *30*, 597.
(9) Roland, C. M.; Ngai, K. L. *Macromolecules* **1992**, *25*, 363.
(10) Pathak, J. A.; Colby, R. H.; Floudas, G.; Jerome, R. *Macromolecules* **1999**, *32*, 2553.
(11) Arbe, A. Alegria, A.; Colmenero, J.; Hoffmann, S.; Willner, L.; Richter, D. *Macromolecules* **1999**, *32*, 7572.
(12) Cendoya, I.; Algeria, A.; Alberdi, J M.; Colmenero, J.; Grimm, H.; Richter, D.; Frick, B. *Macromolecules* **1999**, *32*, 4065.
(13) Urakawa, O.; Fuse, Y.; Hori, H.; Tran-Cong, Q.; Yano, O. *Polymer* **2001**, *42*, 765.
(14) Hirose, Y.; Urakawa, O.; Adachi, K. *Macromolecules* **2003**, *36*, 3699.
(15) Hirose, Y.; Urakawa, O.; Adachi, K. *J. Polym. Sci., Part B: Polym. Phys.* **2004**, *42*, 4084.
(16) Roland, C. M.; Ngai, K. L. *Macromolecules* **1991**, *24*, 2261.
(17) Roovers, J.; Topolowski, P. M. *Macromolecules* **1992**, *25*, 1096, 3454.
(18) Chung, G. C.; Kornfield, J. A.; Smith, S. D. *Macromolecules* **1994**, *27*, 964, 5729.
(19) Lartigue, C.; Guillermo, A.; CohenAddad, J. P. *J. Polym. Sci., Polym. Phys.* **1997**, *35*, 1095.
(20) Min, B. C.; Qiu, X. H.; Ediger, M. D.; Pitsikalis, M.; Hadjichristidis, N. *Macromolecules* **2001**, *34*, 4466.
(21) Lutz, T. R.; He, Y. Y.; Ediger, M. D.; Cao, H. H.; Lin, G. X.; Jones, A. A. *Macromolecules* **2003**, *36*, 1724.
(22) He, Y.; Lutz, T. R.; Ediger, M. D.; Pitsikalis, M.; Hadjichristidis, N.; von Meerwall, E. D. *Macromolecules* **2005**, *38*, 6216.
(23) Ngai, K. L.; Roland, C. M. *Macromolecules* **2004**, *37*, 2817.
(24) He, Y.; Lutz, T. R.; Ediger, M. D. *Macromolecules* **2004**, *37*, 9889.
(25) Shimada, S. *Polym. J.* **1996**, *28*, 647.
(26) Hoffmann, S.; Richter, D.; Arbe, A.; Colmenero, J.; Farago, B. *Appl. Phys. A* **2002**, *74*, S442.
(27) Leroy, E.; Alegria, A.; Colmenero, J. *Macromolecules* **2002**, *35*, 5587.
(28) Adachi, K.; Fujihara, I.; Ishida, Y. *J. Polym. Sci., Polym. Phys. Ed.* **1975**, *13*, 2155.
(29) Hori, H.; Urakawa, O.; Adachi, K. *Polym. J.* **2003**, *35*, 721.
(30) Zhang, S. H.; Jin, X.; Painter, P. C.; Runt, J. *Macromolecules* **2002**, *35*, 3636.
(31) Zhang, S. H.; Painter, P. C.; Runt, J. *Macromolecules* **2002**, *35*, 9403; *Macromolecules* **2004**, *37*, 2636.
(32) Taniguchi, N.; Urakawa, O.; Adachi, K. *Macromolecules* **2004**, *37*, 7832.
(33) Sakaguchi, T.; Urakawa, O.; Adachi, K. *Macromolecules* **2005**, *38*, 422.
(34) Zawada, J. A.; Fuller, G. G.; Colby, R. H.; Fetters, L. J.; Roovers, J. *Macromolecules* **1994**, *27*, 6861.
(35) Gell, C. B.; Krishnamoorti, R.; Kim, E.; Graessley, W. W.; Fetters, L. J. *Rheol. Acta* **1997**, *36*, 217.
(36) Arendt, B. H.; Krishnamoorti, R.; Kornfield, J. A.; Smith, S. D. *Macromolecules* **1997**, *30*, 1127.
(37) Yang, X. P.; Halasa, A.; Hsu, W. L.; Wang, S. Q. *Macromolecules* **2001**, *34*, 8532.
(38) Hayakawa, T.; Adachi, K. *Macromolecules* **2000**, *33*, 6840.
(39) Haley, J. C.; Lodge, T. P.; He, Y.; Lutz, T. R.; Ediger, M. D.; von Meerwall, E. D.; Mijovic, J. *Macromolecules* **2003**, *36*, 6142.
(40) Haley, J. C.; Lodge, T. P. *J. Rheol.* **2004**, *48*, 463.
(41) Haley, J. C.; Lodge, T. P. *J. Chem. Phys.* **2005**, *122*, 234914/1.
(42) Krygier, E.; Lin, G.; Mendes, J.; Mukandela, G.; Azar, D.; Jones, A. A.; Pathak, J. A.; Colby, R. H.; Kumar, S. K.; Floudas, G.; Krishnamoorti, R.; Faust, R. *Macromolecules* **2005**, *38*, 7721.
(43) Pathak, J. A.; Kumar, S. K.; Colby, R. H. *Macromolecules* **2004**, *37*, 6994.
(44) Adachi, K.; Hirano, H. *Macromolecules* **1998**, *31*, 3958.
(45) Schönhals, A. Dielectric Properties of Amorphous Polymers. In *Dielectric Spectroscopy of Polymeric Materials*; Runt, J. P., Fitzgerald, J. J., Eds.; American Chemical Society: Washington, DC, 1997; Chapter 3, pp 81−106.
(46) Roland, C. M.; Paluch, M.; Casalini, R. *J. Polym. Sci., Part B: Polym. Phys.* **2004**, *42*, 4313.
(47) Yamane, M.; Hirose, Y.; Adachi, K. *Macromolecules* **2005**, *38*, 9210; *Macromolecules*, in press.
(48) Roland, C. M.; Ngai, K. L.; Santangelo, P. G.; Qui, X. H.; Ediger M. D.; Plazek, D. J. *Macromolecules* **2001**, *34*, 6159.
(49) Roland, C. M.; Ngai, K. L.; Plazek, D. J. *Macromolecules* **2004**, *37*, 7051.
(50) Urakawa, O.; Swallen, S. F.; Ediger, M. D.; von Meerwall, E. D. *Macromolecules* **2004**, *37*, 1558.
(51) Zetsche, A.; Fischer, E. W. *Acta Polym.* **1994**, *45*, 168.
(52) Kumar, S. K.; Colby, R. H.; Anastasiadis, S. H.; Fytas, G. *J. Chem. Phys.* **1996**, *105*, 3777.
(53) Lodge, T. P.; McLeish, T. C. B. *Macromolecules* **2000**, *33*, 5278.
(54) Halasa, A. F.; Lohr, D. F.; Hall, J. E. *J. Polym. Sci., Polym. Chem. Ed.* **1981**, *19*, 1357.
(55) Stolarzewich, A.; Neugebauer, D. *Macromol. Chem. Phys.* **1999**, *200*, 2467.
(56) Fox, T. G. *Bull. Am. Phys. Soc.* **1956**, *1*, 123.
(57) Kwei, T. K. *J. Polym. Sci., Polym. Lett. Ed.* **1984**, *22*, 307.
(58) Imanishi, Y.; Adachi, K.; Kotaka, T. *J. Chem. Phys.* **1988**, *89*, 7585.
(59) Havriliak, S.; Negami, S. *J. Polym. Sci.* **1966**, *C14*, 99.
(60) Vogel, H. *Phys. Z.* **1921**,*22*, 645.
(61) Fulcher, J. G. *J. Am. Ceram. Soc.* **1925**, *8*, 339.
(62) Matsushima, M.; Fukatsu, M.; Kurata, M. *Bull. Chem. Soc. Jpn.* **1968**, *41*, 2570.
(63) Fetters, L. J.; Lohse, D. J.; Milner, S. T.; Graessley, W. W. *Macromolecules* **1999**, *32*, 6847.
(64) Kyritsis, A.; Pissis, P.; Mai, S.-M.; Booth, C. *Macromolecules* **2000**, *33*, 4581.
(65) Verdier, R. H.; Stockmayer, W. H. *J. Chem. Phys.* **1962**, *36*, 227.
(66) Rouse, P. E. *J. Chem. Phys.* **1953**, *21*, 1272.
(67) Nakazawa, M.; Urakawa, O.; Adachi, K. *Macromolecules* **2000**, *33*, 7898.
(68) Adachi, K.; Imanishi, Y.; Kotaka, T. *J. Chem. Soc., Faraday Trans. 1* **1989**, *85*, 1083.
(69) Hirose, Y.; Adachi, K. *J. Noncryst. Solids*, in press.

MA052216X